

Thermal Control of Melt Flow in Cylindrical Geometries

Gautam Balasubrahmanyam & David Kazmer, University of Massachusetts Lowell

Abstract

The control of plastic freeze-off and melt flow through a cylindrical nozzle is studied. Analysis of the temperature distribution of a nozzle contacting the mold shows a significant temperature distribution as a function of the axial and radial position in the metal and plastic. The temperature of the plastic melt determines the viscosity and subsequent flow through the nozzle. Experimental investigation validates the analysis by characterizing the pressure needed to induce flow as a function of nozzle and mold temperature. Control of the polymer freeze-off and melt flow is necessary for fully automatic production, as well as development of advanced molding processes.

Introduction

The viscosity of a polymer is the single most dominating factor in analyzing the stability of polymer melts in flow geometries. The viscosity is strongly dependent on the temperature and shear rates to which the polymer is exposed. The process of injection molding typically involves high pressures that force the viscous polymer through restricted geometries which results in subjecting the polymer to potentially high shear rates.

Currently the control of the flow behavior of polymers in most cylindrical geometries such as nozzles and gates is passive, which means that the melt temperature distribution and associated flow conductance is governed by a balance of heat convection by the flowing melt with heat conduction from the hot melt to the cold mold. By contrast, active control of the plastic melt can be accomplished through the use of mechanical actuation to cause positive shut-off such as in valve-gates, but is costly and prone to maintenance. It is a goal of on-going research and development to achieve active thermal control of the melt similar to mechanical means. By "active thermal control", it is meant that the temperature of the melt in a narrow cross-section is dynamically manipulated in such a way that the transition from melt flow to freeze-off and from freeze-off to melt flow occurs quickly with respect to the process dynamics to accomplish some goal that governs production efficiency and molded part quality.

As a first step towards accomplishing active thermal control, this paper analyzes the temperature distribution in nozzles and characterizes the viscosity-shear rate behavior of the melt in cylindrical geometries. Then, actuation requirements for temperature and pressure are examined to guarantee a transition from freeze-off and melt flow.

Rheological Characterization and Modeling

Stability of polymer melts can be estimated by both numerical simulation and physical experimentation. Numerical simulation of injection molding requires viscosity data that covers the temperatures and shear rates encountered in the process. The two most popular devices for obtaining such data are the capillary rheometer and the oscillatory cone and plate or parallel plate rheometer. Both these devices are capable of providing information suitable for injection molding simulation [1].

The capillary rheometer is the most widely used instrument employed for viscosity characterization. The capillary rheometer has the capability of replicating the pressures, rates and flow fields encountered in cylindrical geometries. The rheological quantities that can be obtained from experimental pressure and volumetric flow rate data are the apparent viscosity, η_a (Equation 1) and the apparent shear rate, $\dot{\gamma}_a$ (Equation 2) [1]:

$$\eta_a = \frac{\Delta P}{\Delta L} \frac{\pi R^4}{2Q} \quad (1)$$

$$\dot{\gamma}_a = \frac{4Q}{\pi R^3} \quad (2)$$

where Q is the volumetric flow rate, R is the capillary radius, ΔL is the capillary length, and ΔP is the pressure drop across capillary.

Fitting of experimental data to the models such as the second order polynomial and the Cross model (with WLF temperature dependence) can be employed as a reasonable technique to predict the shear rate of the polymer and hence its behavior in the injection molding process. The Cross model with WLF temperature dependence is:

$$\eta = \frac{\eta_0}{1 + \left(\frac{\eta_0 \dot{\gamma}}{\tau^*} \right)^{1-n}} \quad (3)$$

and

$$\eta_0 = D_1 \exp \left[- \frac{A_1 (T - T^*)}{A_2 + (T - T^*)} \right] \quad (4)$$

where D_1 , A_1 , A_2 , τ^* are WLF model coefficients [2].

Experimental

In order to actively control the flow of the polymer melt in cylindrical geometries, accurate rheological characterization of the polymer at low temperatures was

necessary. Therefore, the viscosity and shear rate data were obtained on commercial polystyrene resin (Styron 678C, Dow Plastics) using a Kayeness Galaxy V capillary rheometer. Measurements were made using a capillary with a diameter of 1mm and L/D ratio of 20:1. Data were obtained at temperatures in the range of 150-210°C, much lower than the typical processing temperatures 180-260°C.

Figure 1 shows the effect of temperature on average flow rate of the melt through the capillary at different pressures. Due to extremely high melt viscosities, it was not possible to acquire rheological data for the material at lower values of temperature and pressure than was tested with this device. The data obtained from the low temperature testing was fitted to the Cross-WLF model, and is provided in Table 1. Table 1 also provides the published Cross-WLF coefficients obtained from Moldflow.

Figures 2 and 3 plot the viscosity versus shear rate behavior for this resin from Moldflow's material database and for the fitting of the low temperature data, respectively. As can be seen for the same range of shear rates, the model fit to the low temperature test data results in higher predicted viscosity compared to Moldflow's model. The low temperature data is more accurate at low temperatures, since it is derived from the processing conditions of interest. In fact, the Moldflow model was probably derived from rheology data closer to the center of the specified melt temperature range (e.g. 200, 220, and 240C). Moldflow's under prediction of melt viscosity at low temperatures might be expected, since the dependence of the melt viscosity is non-linear with temperature, and at lower temperatures there is increased sensitivity. This data is also consistent with that of Sherbelis and Friedl [2].

To investigate this phenomenon, Figure 4 plots the zero shear viscosity versus temperature for models from Moldflow and the test data. It can be seen that at higher temperatures the two models converge. But at lower temperatures, which govern the no-flow condition, the models diverge significantly. In fact, at 140C Moldflow under predicts the viscosity by a factor of 8. At 120C, where the true viscosity is unknown, the two models differ by a factor of 9000. However, it is across this regime that the polymer melt becomes solid, and this paper assumes that the model derived from the low temperature is more accurate.

Figure 5 shows the assembly of the nozzle, sprue and mold plate along with the polymer in the form of a revolved geometry. The model was designed using Pro-Engineer. In order to estimate the temperature distribution of the melt along the nozzle when it is in contact with the sprue bushing, an axisymmetric finite element analysis was carried out in Pro-Mechanica. It is observed that a circular cooling line layout is modeled. While non-circular cooling lines are mostly used in practice, this modeling approach provides a close approximation while allowing vastly reduced computation times and finer mesh density.

The nozzle temperature was set to 250°C, the mold coolant temperature to 50°C with a heat transfer coefficient

of 10 W/m²K. Steel was chosen as the material for the nozzle, sprue, and mold plate while polystyrene was selected as the polymer material. Figure 6 shows the results of the steady state temperature analysis. The model here is represented in a two dimensional axisymmetric form, showing the temperature gradients in a cross-section of the nozzle and mold. As can be seen from Figure 6 there is a significant variation of temperature across the length of the nozzle. Since the rheological behavior is critically dependent on the temperature, this temperature gradient could lead to inconsistent behavior of the melt along the length of the nozzle. Any active thermal control system would strategically provide additional heat to bring about uniform temperatures and enable flow.

The rheological behavior and the temperature distribution predicted via experimentation are used to evaluate the control of the plastic melt and freeze-off in cylindrical geometries. In order to predict the viscosity at lower temperatures and pressures the equations for continuity and momentum are solved by numerical integration as per standard simulation practice [3]. In this analysis, the equation for conservation of energy is not utilized since this investigation is only focused on the initial response of flow at low flow rates, with the initial condition is provided by the steady state heat conduction analysis. As such, there is no need to model transient convection or conduction or viscous generation since the polymer will continue to flow once melt flow is initiated. For those readers with interest in investigating the thermal transients associated with high rates of polymer deformation, the authors would suggest Pearson [4].

Results and Discussion

It has been observed that some residual pressure has been maintained in the barrel of injection molding machines after plastication and even after decompression. This pressure is typically on the order of 100 psi, and may be due to the thermal expansion and creeping flow of the plasticating material in the screw, body forces and relaxation of the accrued shot, or idling control signals from the molding machine. The objective of this research is to provide a thermal control device that guarantees freeze-off during plastication and mold open, but readily admits flow during in the filling and packing stages. To efficiently and rapidly control the flow of freeze-off and flow of the polymer melt, we desire to change the temperature by a small amount across which the flow conductance of the polymer is greatly increased.

The results of this paper were acquired through non-Newtonian simulation of the melt flow according to the mass and momentum equations [3]. It should be noted that for Newtonian flows, the temperature profiles obtained in Figure 6 can be utilized to estimate the pressure drop across the nozzle according to the relation:

$$\Delta P = \sum_{i=1}^n \eta(T_i) \Delta L_i \left(\frac{2Q}{\pi R^4} \right) \quad (5)$$

where, T_i and L_i are the temperature and the length of an element of polymer melt in the nozzle.

Figure 7 plots the flow rate through the nozzle at varying reference temperatures and pressures. The log of flow rate is plotted given the significant increase in the flow rate with increases in melt temperature or injection pressure. Point 1 in the figure establishes a baseline no-flow condition of 0.001 cc/min at a melt temperature of 130 C and a pressure drop across the nozzle of 1 MPa. Such a no-flow condition may be specified to guarantee the prevention of leakage during plastication or a mold open condition. It should be noted that the no-flow condition may be made even more conservative by requiring a lower melt temperature to prevent leakage at high pressure drops.

To enable melt flow, it is necessary to either increase the melt temperature in the nozzle or apply a much greater pressure drop. Once melt flow is induced, the convection of the heated melt and internal viscous dissipation will further increase the bulk melt temperature, thereby further increasing the flow conductance and sustaining continued melt flow. The primary issue, then, is how to best enable initial melt flow. Most molding practitioners have observed attempts to clear a plugged nozzle or gate by increasing the injection pressure. Depending on the geometry of the gate and temperature distributions, these attempts can lead to a clear gate at relatively low applied pressure, a bullet exit at relatively high applied pressure, or no clearance at any pressure.

Assume for now that a flow rate of 0.1 cc/min is needed to initialize steady flow through the nozzle. While not shown in Figure 7, the analysis indicates that a pressure of approximately 100 MPa will be required to accomplish a flow rate of 0.1 cc/min while maintaining the temperature at 130 C. Alternatively, consider points 2 and 3 provided in Figure 7. Point 2 indicates that 0.1 cc/min of flow can be accomplished with very low pressure (0.1 MPa) by increasing the melt temperature from 130 to 170C. Alternatively, point 3 indicates that the same flow rate can be accomplished by increasing the melt temperature from 130 to 140C and the injection pressure from 1.0 to 2.5 MPa.

From the point of view of thermal actuation, point 3 is highly preferred to point 2. Specifically, the energy required to increase the melt temperature is defined as:

$$E = \varepsilon m C_p \Delta T \quad (6)$$

where m is the mass of the polymer, C_p is the heat capacity of the polymer, ΔT is the required temperature change of the melt, and ε is the actuation efficiency (percentage of heater power that enters the melt, dependent on nozzle and heater geometry and thermal properties) on the order of 10%. To reduce actuation energy and response time, it is clearly desirable to reduce the diameter of the nozzle as well as the required temperature change. However, reducing the diameter will further reduce both the initial and steady state flow conductance, such that the minimum diameter is dictated by the maximum allowable pressure drop across the nozzle during the filling stage.

If the nozzle diameter is 6 mm in diameter (0.25 inches) and 6 mm in length, then the energy required for a 10 C temperature increase is approximately 25 J. While there are many different heater technologies, a realistic heater power density of 100 W/in² is readily obtained. In this geometry, this corresponds to a heater of 17W. Such a heater would require approximately 1 second to actively raise the melt temperature in the nozzle by 10C. Clearly, further increases in melt temperature would require proportionally greater power and longer heating times. While a 1 second delay during mold closure would likely not extend the cycle time of most molding processes, a 5 or 10 second cycle time would be economically crippling.

As such, the successful development of active thermal control in cylindrical geometries is dependent on the proper identification of the baseline no-flow temperature as well as the minimum temperature and pressure change required to guarantee control of freeze-off and melt flow. Towards this objective, a melt stability index has been defined to compare the flow when "on" (high temperature, high pressure condition) to flow when "off" (low temperature, low pressure). The stability index (I_s) can be expressed as:

$$I_s = \log \left(\frac{Q_{on}}{Q_{off}} \right) \quad (7)$$

Figure 8 shows the stability index as a function of the temperature change and pressure change. In this case the flow rate for the "off" condition is that at a temperature of 120°C and pressure of 0.1 MPa. For reference points 1, 2, and 3 from Figure 7 are also provided in Figure 8. A stability index of 2 indicates that the initial flow rate when "on" is 100 times greater than the flow rate when "off" as in the previously example. It is observed that the combination of a 50C temperature change and a 2.5 MPa pressure change provides a stability index of 8, which corresponds to an increase in the in melt flow of 10,000,000,000%. This magnitude increase is certainly sufficient to guarantee a transition from freeze-off to melt flow across a wide range of polymeric materials.

Conclusions

The injection molding process would be greatly benefited by the use of active thermal control in cylindrical geometries such as nozzles and gates. This paper examined the rheological, melt flow, and freeze-off behavior for a polystyrene resin. A stability index was proposed that compares the flow rates in "on" and "off" conditions. The analysis indicated that relatively small changes in melt temperature and injection pressure can substantially increase the flow conductance and dynamically control the onset of melt flow.

To enable the utilization of an active thermal control for injection molding, further work is required in two areas. First, it is necessary to better specify and validate the required operating temperature and pressure changes for various amorphous and semi-crystalline resins. Second, these specifications should lead to a set of design and

processing guidelines, which allow the automatic operation of the developed thermal actuators based solely on reference values for the glass transition temperature and temperature sensitivity which can be obtained from standard material databases.

Acknowledgements

The authors would like ThermoCeramix for sponsoring this research. We would also like to thank Dr. Bingfeng Fan for fitting the Cross model to the experimental data and identifying an outlier.

References

- [1] Kazmer, D. O. and J. S. Willey, *An Examination of Material Characterization and Modeling Techniques for Injection Molding Simulation*, Annual technical conference 1992, p. 958-964.
- [2] Sherbelis, G. and C. Friedl, *The Importance of Low Temperature Viscosity to CAE Injection Molding Simulation*, Annual technical conference 1992, p. 954 – 957.
- [3] Fan, B. and D. Kazmer, *Simulation of Optical Media Molding*, Annual Technical Conference: Injection Molding Division. 2003 Nashville, TN.
- [4] Pearson, J. R. A., *Polymer Flows Dominated by High Heat Generation and Low Heat Transfer*, Polymer Engineering and Science, v. 18, n. 3, p. 222-229.

Table 1: Cross-WLF coefficients for Moldflow and acquired data

Cross-WLF coefficients	MF	New Fit
n	0.2903	0.2718941
τ^* (Pa)	13678	35270.99
D_1 (Pa-s)	7.44E+10	2.94817E+16
D_2 (K)	373.15	379.1202
D_3 (K/Pa)	0	0
A_1	25.971	35.25966
A_2 (K)	51.6	20.09128

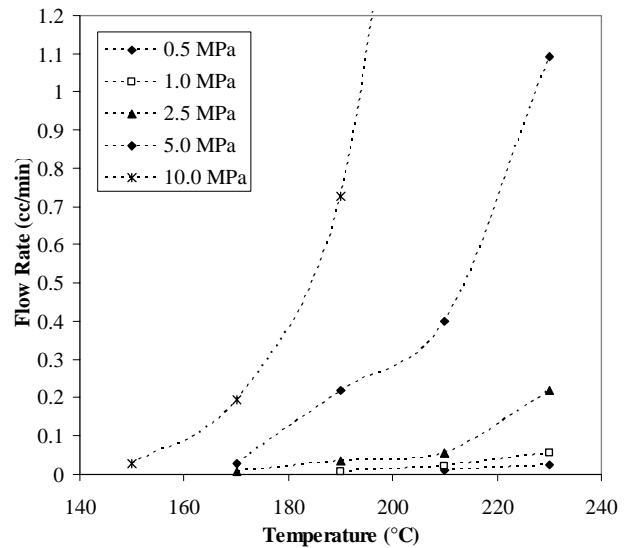


Figure 1: Flow rate versus temperature and pressure for Styron 678C

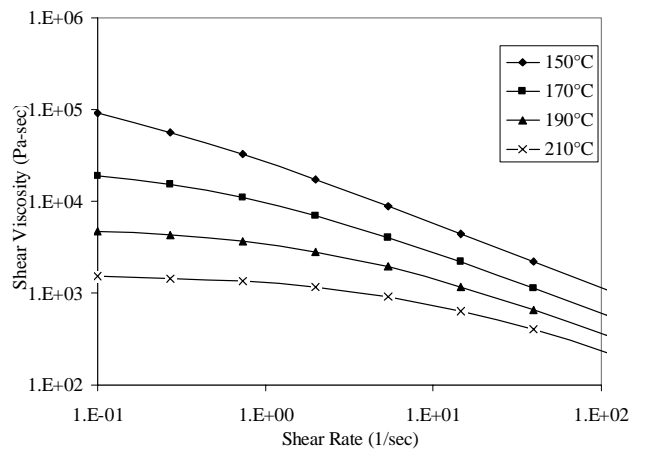


Figure 2: Predicted apparent viscosity using the Cross-WLF model with Moldflow's coefficients

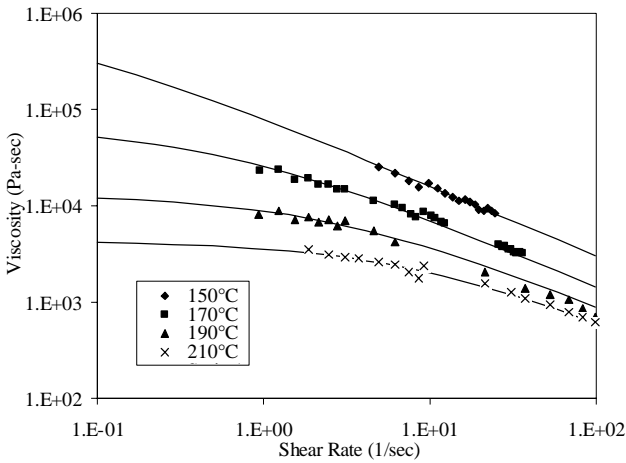


Figure 3: Observed and predicted apparent viscosity using the Cross-WLF fit at low temperatures

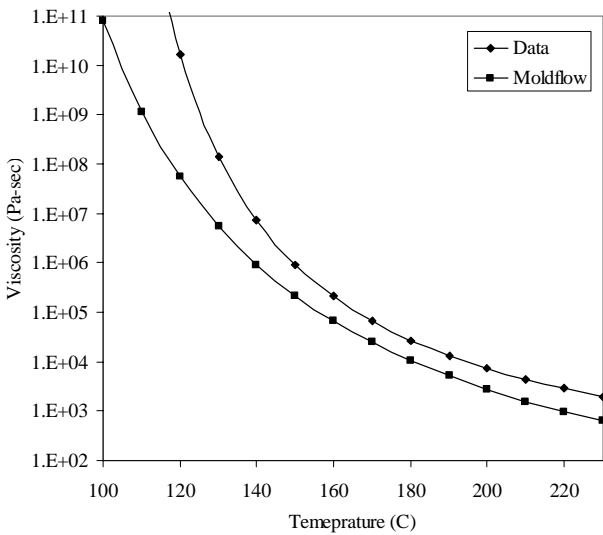


Figure 4: Zero shear rate viscosity versus temperature for Moldflow and low temperature coefficients

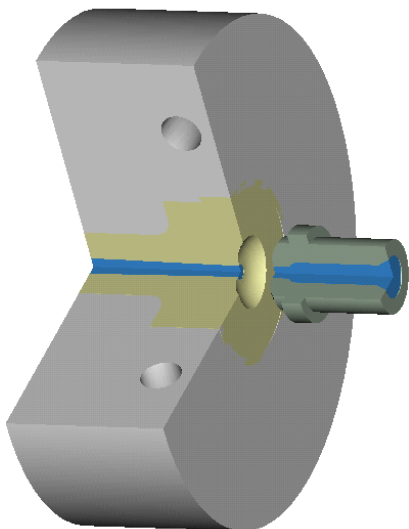


Figure 5: Mold and nozzle assembly

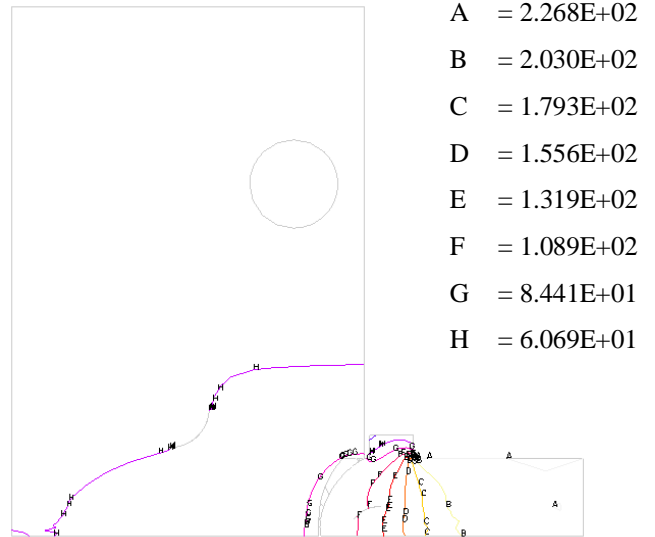


Figure 6: Temperature (°C) distribution across the assembly

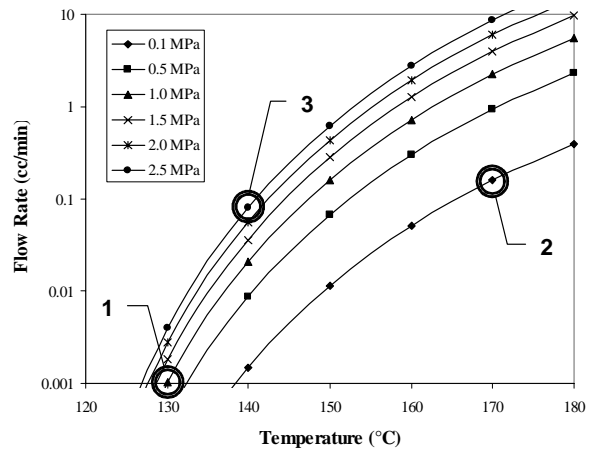


Figure 7: Effect of temperature and pressure on the average flow rate

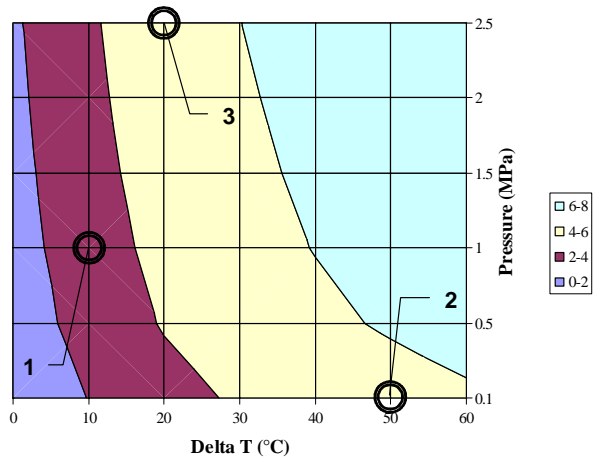


Figure 8: Stability index as a function of temperature and pressure change